

# Study of the conversion of the VO to the VO<sub>2</sub> defect in silicon heat-treated under uniform stress conditions

C. A. Londos<sup>a)</sup>

*University of Athens, Physics Department, Solid State Section, Panepistimiopolis, Zografos, Athens 157 84, Greece*

I. V. Antonova

*Institute of Semiconductor Physics, Pr. Lavrentyeva 13, 630090, Novosibirsk, Russia*

M. Potsidou

*University of Athens, Physics Department, Solid State Section, Panepistimiopolis, Zografos, Athens 157 84, Greece*

A. Misiuk

*Institute of Electron Technology, Al. Lotnikow 32/46, 02-668 Warsaw, Poland*

J. Bak-Misiuk

*Institute of Physics, Polish Academy of Sciences, Al. Lotnikow 46, 02-668 Warsaw, Poland*

A. K. Gutacovskii

*Institute of Semiconductor Physics, Pr. Lavrentyeva 13, 630090, Novosibirsk, Russia*

(Received 6 June 2001; accepted for publication 5 November 2001)

The VO defect is one of the major defects produced by irradiation in Cz-grown Si. Its presence in the infrared spectra is manifested by a localized vibration mode (LVM) band at 829 cm<sup>-1</sup>. Upon annealing, the decay of this band is accompanied by the emergence in the spectra of another LVM band at 890 cm<sup>-1</sup> generally attributed to the VO<sub>2</sub> defect. The annealing of the VO center is discussed in the literature by considering mainly two reaction processes in neutron irradiated material, that is, VO + Si<sub>I</sub> → O<sub>i</sub> and VO + O<sub>i</sub> → VO<sub>2</sub>, which could occur in parallel. There are some points, however, which cannot be explained within the above reaction scheme. In this article we report infrared, x-ray, transmission electron microscopy and selective etching investigations on the annealing behavior of the VO defect, in neutron-irradiated Cz-grown Si samples, subjected to various high temperature–high pressure (HTHP) treatments prior to the irradiation. The contribution of each of the above two reactions to the whole annealing process of the VO defect and its conversion to the VO<sub>2</sub> defect is studied. The results are discussed by taking into account that the state of the self-interstitials, adjacent to the oxygen precipitates and the structural defects formed due to the HTHP treatment, is different for each sample because of the different treatments.

© 2002 American Institute of Physics. [DOI: 10.1063/1.1430529]

## INTRODUCTION

The scope of the study of radiation-induced defects and their interaction with lattice defects and impurities present in the substrate is generally twofold. First, for the purpose of knowing and understanding the nature, the properties, the mechanisms of the formation of the defects, and their interactions, and second, because it is necessary, with the help of the acquired knowledge, to control the yield and improve the performance of the corresponding devices. This is particularly important for silicon, which is the basic material for electronic devices. A-centers are created as the dominant defects in Cz-Si, by any kind of irradiation. The main reason is that the silicon monovacancies *V* produced by irradiation are mobile at room temperature, and besides annihilation by silicon interstitials, or by pairing with each other to produce divacancies *V*<sub>2</sub> are trapped by interstitial oxygen atoms *O*<sub>i</sub> to form vacancy–oxygen pairs VO, the well-known A-centers.

The presence of such pairs in Cz-Si is manifested by an infrared absorption band at 828 cm<sup>-1</sup>. They are stable up to ~300 °C. Annealing at this temperature results in the decrease in the intensity of the 828 cm<sup>-1</sup> band, which is correlated with the growth of another absorption band at 890 cm<sup>-1</sup>, generally attributed to the VO<sub>2</sub> defect.<sup>1,2</sup> Other defects are also formed at these temperatures.<sup>3</sup>

However, there are some points<sup>4</sup> in the whole behavior of the 890 cm<sup>-1</sup> band that cannot easily fall into the picture of the assignment of this band to the VO<sub>2</sub> defect. Such a point is, for instance,<sup>5</sup> the failure in detecting isotopic splitting for the defect in <sup>16</sup>O and <sup>18</sup>O implanted silicon samples. Most of the experimental results, concerning the decay of the 828 cm<sup>-1</sup> band and the growth of the 890 cm<sup>-1</sup> band could be understood by mainly considering<sup>6</sup> the reactions VO + Si<sub>I</sub> → O<sub>i</sub> and VO + O<sub>I</sub> → VO<sub>2</sub>, which should be held in parallel, at least in a part of the whole annealing process. However, there is data that could not easily fit the above picture. More specifically, the analysis of the annealing data concerning the loss of the VO center indicates processes<sup>7</sup> leading to

<sup>a)</sup>Electronic mail: hlontos@cc.uoa.gr

a local rearrangement of the defect, which is not easily reconciled with the above reaction scheme. Thus the phenomenon is not fully understood. In addition, the degree of the contribution of each one of the above two reactions to the annealing of the VO defect and the growth of the VO<sub>2</sub> defect is another issue pending investigation.

It is well-established in the literature<sup>8,9</sup> that heat treatments of silicon at various temperatures lead to the formation of thermal donors, oxygen precipitates, and various structural defects, as, for example, rod-like defects, dislocations, stacking faults, etc. The presence of these defects is expected to affect the annealing behavior of radiation-induced defects, since the environment, where the various processes take place, has been changed. Noticeably, the concentration of interstitial oxygen,  $N_{\text{O}}$ , in heat-treated samples is decreased due to the oxygen precipitation. Concerning the VO defect, investigations<sup>10</sup> of its behavior on samples subjected to pre-heat treatments have shown substantial changes in the annealing temperature of this center. It has been concluded that oxygen-related precipitates and structural defects, which can trap and release vacancies and self-interstitials, have a profound effect in the annealing temperature of the A-centers. Note that the clustering and precipitation of oxygen in silicon is accompanied<sup>11</sup> by the emission of self-interstitials, which are expected<sup>12</sup> to aggregate adjacent to the precipitates.

On the other hand, the application of hydrostatic stress can induce<sup>13</sup> changes in the structure of the defects. More specifically, the application of uniform stress at various temperatures has<sup>14</sup> significant influence on the concentration of interstitial oxygen and generally on the concentration of the structural defects formed. It has also been demonstrated<sup>14</sup> that high temperature–high pressure (HTHP) treatments result in an enhanced concentration of very small defects, detected only in x-ray reciprocal lattice maps. It is therefore expected that treatments of Si crystals under various HTHP treatments would affect the annealing behavior of the VO defect. The study of this phenomenon is the main object of this work. We shall also try to answer the following question. Is it the decrease in the concentration of interstitial oxygen due to the precipitation or is it the structural defects formed that have a greater impact on the annealing behavior of the VO defect?

## EXPERIMENTAL DETAILS

Six samples cut from a 2 mm thick, 001 oriented Si wafer were used. The material was *p*-typed, boron doped with resistivity  $\rho \approx 9 \Omega \text{ cm}$  ( $[B] \approx 1.3 \times 10^{15} \text{ cm}^{-3}$ ). Their initial oxygen concentration was  $[O_i]_0 \sim 8.3 \times 10^{17} \text{ cm}^{-3}$ . The samples were subjected to various combinations of HTHP treatments as shown in Table I and then irradiated by fast neutrons to a fluence of  $\sim 1 \times 10^{17} \text{ cm}^{-2}$  at  $T \approx 50^\circ \text{C}$ . Afterwards, they were subjected to a heat treatment at  $220^\circ \text{C}$  for 150 min aiming at a complete annealing of the large cluster of defects and disordered regions, present in neutron-irradiated material. As it is expected<sup>3</sup> this process resulted in changes in the VO and the  $[O_i]$  intensities due to the liberation of vacancies, which react with oxygen atoms to form additional VO centers. The establishing values of the  $O_i$  con-

TABLE I. The oxygen interstitial concentration, the  $N_{\text{VO}}$  and the  $N_{\text{VO}_2}$  intensities, and the intensity ratio  $N_{\text{VO}}/N_{\text{VO}_2}$  for the various samples, respectively.

Sample	A	B	C	D
$T(^{\circ}\text{C}), P(\text{kbar}), t(\text{h})$	$[O_i] \times 10^{17}$	$N_{\text{VO}}$ (arb. units)	$N_{\text{VO}_2}$ (arb. units)	$N_{\text{VO}}/N_{\text{VO}_2}$
S1 untreated	7.78	0.0788	0.0380	2.074
S2 900,3,3	7.71	0.0771	0.0370	2.084
S3 900,12,5	5.95	0.0681	0.0228	2.987
S4 1027,12,5	4.82	0.0612	0.0172	2.363
S5 900,12,10	3.91	0.0424	0.0105	4.038
S6 957,12,10	3.02	0.0304	0.0042	7.238

centration and the VO intensity after this process are also shown in Table I. Finally, the samples were subjected to a heat treatment at  $400^\circ \text{C}$ , for 4 h, for the purpose of complete conversion of the VO to the VO<sub>2</sub> defects. Infrared spectra were taken at room temperature by a dispersive kind of spectrometer. X-ray investigations were performed using a high-resolution diffractometer in double configuration. Rocking curves and reciprocal space maps were recorded for all samples. A high-resolution experimental setup was realized by employing a four-crystal Ge (220) Bartels-type monochromator in the primary beam and a channel-cut double-reflection Ge (220) analyzer in the diffracted beam. Selective etching measurements were performed in the Sirtle solution (33%CrO<sub>3</sub>: HF in proportion 1:2) for 5 min. Transmission electron microscopy (TEM) measurements were also carried out on the samples in the course of this investigation.

## RESULTS AND DISCUSSION

Dots in Fig. 1 represent experimental results showing the variations of the intensities of (a) the VO defect, (b) the VO<sub>2</sub> defect, and (c) the intensity ratio  $N_{\text{VO}}/N_{\text{VO}_2}$  versus the oxygen concentration of the samples prior to the annealing stage at  $400^\circ \text{C}$  for 4 h. Notice that the intensity ratio  $N_{\text{VO}}/N_{\text{VO}_2}$  is not the same for the various samples. In the following we shall try to understand the above exhibiting behavior first by modeling of the anneals and then by considering the effects of the various HTHP pretreatments on the annealing curves.

The most important reactions occurring during the decay of the VO defect and the growth of the VO<sub>2</sub> defect are the following:



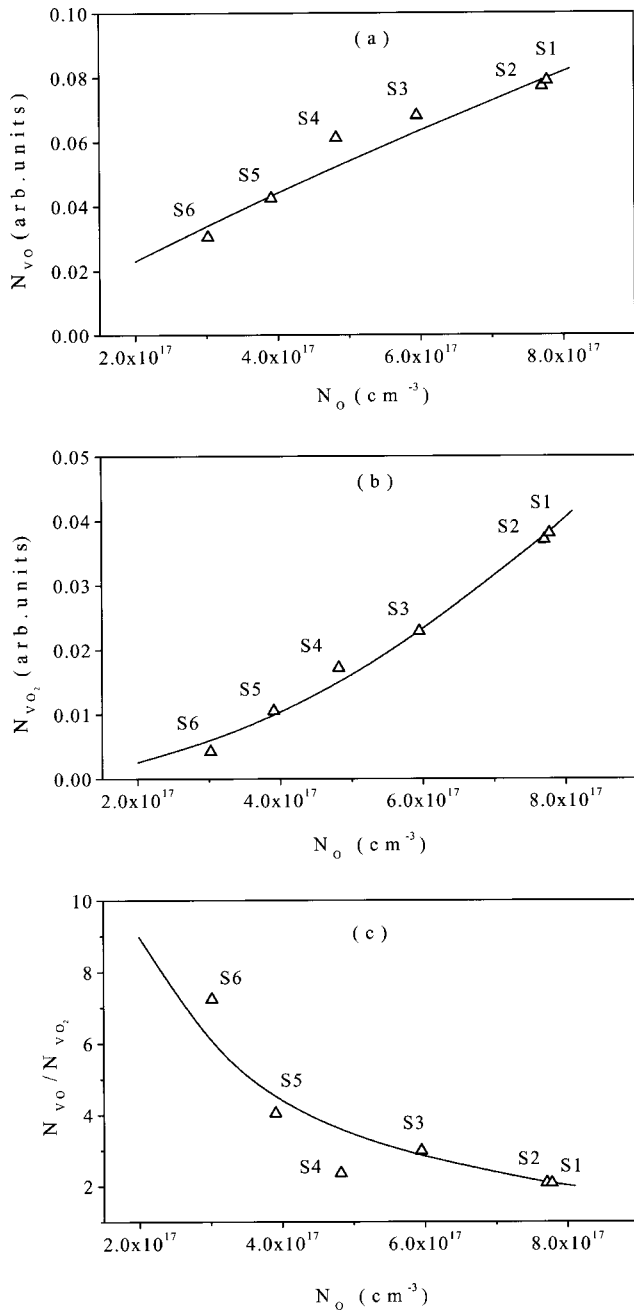


FIG. 1. (a) and (b) The variation of the VO concentration ( $N_{VO}$ ) and the  $VO_2$  concentration ( $N_{VO_2}$ ) of each sample vs the oxygen concentration ( $N_O$ ) prior to the conversion of the VO defect to the  $VO_2$  defect. (c) The variation of the  $N_{VO}/N_{VO_2}$  ratio of each sample correspondingly vs  $N_O$ .



where  $k_1$ ,  $k_2$ ,  $k_3$ ,  $k_4$ , and  $k_5$  are the rate constants characterizing each one of the above reactions, respectively. We assume that Eqs. (1)–(5) constitute a more or less complete reaction scheme describing the phenomenon. Thus the whole process concerning the VO and the  $VO_2$  defects is represented correspondingly by the following rate reactions:

$$\frac{dN_{VO}}{dt} = k_4 N_O N_V - k_1 N_{VO} N_{Si_I} - k_2 N_{VO} N_O - k_3 N_{VO} N_V, \quad (6)$$

$$\frac{dN_{VO_2}}{dt} = k_2 N_{VO} N_O - k_5 N_{VO_2} N_{Si_I}. \quad (7)$$

In the steady state, the concentrations are given by the equations

$$k_4 N_O N_V - k_1 N_{VO} N_{Si_I} - k_2 N_{VO} N_O - k_3 N_{VO} N_V = 0, \quad (8)$$

$$k_2 N_{VO} N_O - k_5 N_{VO_2} N_{Si_I} = 0, \quad (9)$$

from which we receive

$$N_{VO} = \frac{k_4 N_V N_O}{k_1 N_{Si_I} + k_2 N_O + k_3 N_V}, \quad (10)$$

$$N_{VO_2} = \frac{k_2 N_{VO} N_O}{k_5 N_{Si_I}}. \quad (11)$$

Putting  $k_2/(k_4 N_V) = \alpha_1$  and  $(k_1 N_{Si_I} + k_3 N_V)/k_4 N_V = a_2$ , Eq. (10) becomes

$$N_{VO} = \frac{N_O}{a_1 N_O + a_2}. \quad (12)$$

Upon replacing Eq. (12) with Eq. (11) and putting  $\alpha_1 k_5 N_{Si_I}/k_2 = \alpha_3$  and  $\alpha_2 k_5 N_{Si_I}/k_2 = \alpha_4$ , we get

$$N_{VO_2} = \frac{N_O^2}{a_3 N_O + a_4}. \quad (13)$$

Upon dividing Eqs. (12) and (13) we get

$$\frac{N_{VO}}{N_{VO_2}} = \frac{a_3 N_O + a_4}{a_1 N_O^2 + a_2 N_O}. \quad (14)$$

We have solved numerically Eqs. (12)–(14) and the results for parameters  $\alpha_1 = 1.833$ ,  $\alpha_2 = 8.333 \times 10^{18}$ ,  $\alpha_3 = 3.45 \times 10^{18}$ , and  $\alpha_4 = 1.555 \times 10^{37}$  are depicted in the Figs. 1(a)–1(c) as curves for the  $N_{VO}$ ,  $N_{VO_2}$ , and the ratio  $N_{VO}/N_{VO_2}$ , respectively, versus the oxygen concentration of each sample prior to the (400 °C, 4 h) annealing stage. The chosen values for the parameters  $\alpha_1$ ,  $\alpha_2$ ,  $\alpha_3$ , and  $\alpha_4$  are the most appropriate in order to obtain best fit curves for the experimental results. Apparently, it is reasonable to discuss the relations between the rate constants of the reactions (1)–(5) for the used values of the parameters  $\alpha_1$ ,  $\alpha_2$ ,  $\alpha_3$ , and  $\alpha_4$ . In the following we shall assume that  $N_V$  and  $N_{Si_I}$  are of the same order of magnitude. From the relation  $k_2/(k_4 N_V) = \alpha_1$  and by considering  $N_V$  and  $N_{Si_I}$  of the order of  $5 \times 10^{16}$ , the selected value of  $\alpha_1 = 1.833$  leads to  $k_2/k_4 = 9.165 \times 10^{16}$ . This means that the rate constant of reaction (2) is much larger than that of reaction (4). From the relation  $\alpha_1 k_5 N_{Si_I}/k_2 = \alpha_3$ , the selected value  $\alpha_3 = 3.45 \times 10^{18}$  leads to  $k_5/k_2 = 37$ . This means that the rate constant of reaction (5) is larger by one order of magnitude than that of reaction (2). The same value for the ratio  $k_5/k_2$  is also obtained from the relation  $\alpha_2 k_5 N_{Si_I}/k_2 = \alpha_4$ , when selecting  $\alpha_4 = 1.555 \times 10^{37}$  and  $\alpha_2 = 8.333 \times 10^{18}$ . Notice that the values of the parameters  $\alpha_1$ ,  $\alpha_2$ ,  $\alpha_3$ , and  $\alpha_4$  are compatible with the relation  $\alpha_1/\alpha_2 = \alpha_3/\alpha_4$ , as expected from the expressions of the parameters  $\alpha_3$  and  $\alpha_4$ . Finally, by combining the relations  $k_2/(k_4 N_V) = \alpha_1$  and  $(k_1 N_{Si_I} + k_3 N_V)/k_4 N_V = a_2$ , we

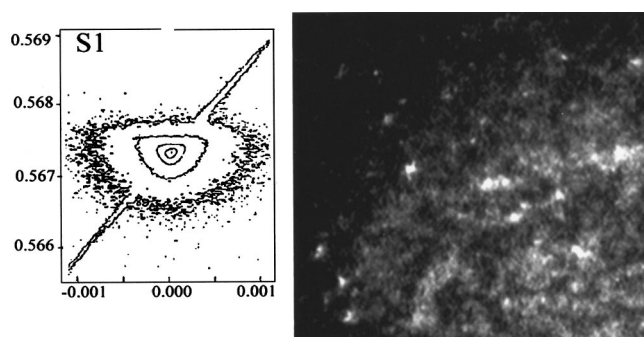


FIG. 2. Reciprocal space map around the 004 reciprocal space point (left) and plan-view TEM image (right) for a nontreated  $S_1$  sample. The axes are marked in  $\lambda/2d$  units,  $\lambda$  is wavelength and  $d$  is lattice interplanar distance. TEM image size is  $0.2 \times 0.15 \mu\text{m}$ .

get the relation  $(k_1 + k_3)\alpha_1 N_V/k_2 = \alpha_2$ , which leads to the relation  $(k_1 + k_3)/k_2 = 91$ , showing that the sum of the rate constants of reactions (1) and (3) is larger, by approximately one order of magnitude, than that of reaction (2). As one can see from the figures, the experimental results do not exactly fit the theoretical ones, especially for the VO. It means that it is necessary to take into account that the HTHP treatments of the samples before irradiation do not only lead to a decrease in the oxygen concentration but also to changes in the structural defects, which act as sinks for vacancies and interstitials.

Physically the decay of the VO defect occurs<sup>2</sup> mainly through the destruction of the VO by the self-interstitials [Eq. (1)] and the coupling of the VO with  $O_i$  for the production of the  $VO_2$  defect [Eq. (2)]. The first reaction depends on the number of the self-interstitials being present at the aggregates adjacent to the interface of the oxygen precipitates and the Si matrix and their ability to release from these aggregates. If one assumes that the activation energy for the liberation of the self-interstitials in order to break away from the agglomerates is smaller than the activation energy for the movement of the VO defect and its subsequent trapping by an  $O_i$  atom to form the  $VO_2$  defect, then the reaction  $VO + Si_I \rightarrow O_i$  occurs earlier than the reaction  $VO + O_i \rightarrow VO_2$ . Of course, there appears no reason why both reactions cannot operate in parallel, at least for a part of the annealing process. Notice that the first reaction will stop when the supply of self-interstitials is ceased. On the other hand, the number of self-interstitials and their ability to participate in the reactions depends on the form, the shape, and the density of the oxygen precipitates and the interstitial-type defects (i.e., dislocation loops), which in turn depend on the HTHP treatment performed on each sample before irradiation. This means that the effectiveness of the reaction  $VO + Si_I \rightarrow O_i$  changes according to the treatment each sample has been given. Therefore the number of VO defects reacting with the  $O_i$  atoms for producing the  $VO_2$  defects is different for each sample. In other words, the ratio  $N_{VO}/N_{VO_2}$  is expected to be different for each sample due to the different HTHP treatments. This was observed experimentally [Fig. 1(c)].

Let us now concentrate on the defects formed in the investigated samples as a result of the HTHP treatments and subsequent neutron irradiation. Figure 2 shows reciprocal

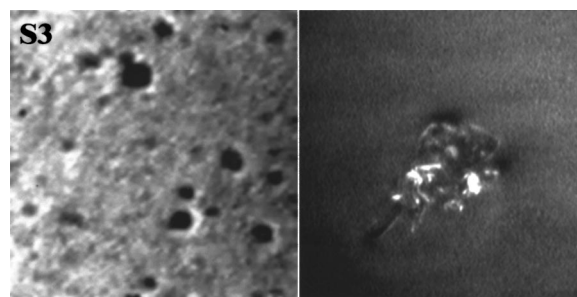


FIG. 3. Surface image after selective etching (left) and plan-view TEM image (right) for sample  $S_3$  treated at  $900^\circ\text{C}$  for 5 h at 1.2 GPa. TEM image size is  $1 \times 0.75 \mu\text{m}$ .

space maps around the 004 reciprocal space point and plan-view TEM image of the untreated sample  $S_1$ . Small stressed areas are observed in the TEM image. Reciprocal space maps also show considerable concentration of defects or stressed areas in the sample. The observed stressed areas are most likely related to clusters of defects introduced by neutron irradiation and subsequent annealing. We notice that selective etching measurements on this sample showed no defects present.

Selective etching studies of the samples  $S_2$  and  $S_3$  show the appearance of hillocks (oxygen precipitates) on their surface. The increase in the applied pressure and the time duration of the treatment leads to the increase in the hillock size. The image of the  $S_3$  sample surface after selective etching and the TEM image of this sample are given in Fig. 3. Small stressed areas do not appear in the TEM image, although relatively large oxygen precipitates with dislocation loops around them are seen. The oxygen precipitate density is found from selective etching measurements to be about  $2 \times 10^6$  and  $2.5 \times 10^6 \text{ cm}^{-2}$  for samples  $S_2$  and  $S_3$ , correspondingly.

TEM images of samples  $S_4$ ,  $S_5$ , and  $S_6$  also show the oxygen precipitates surrounded by dislocation loops (see Fig. 4). The increase in the temperature and/or the time duration of the HTHP treatment leads to the increase in size of the dislocation loops. The same observations come from  $x$ -ray reciprocal space maps on these samples (Fig. 4) while the defect dimensions increase. Selective etching studies show the appearance of small defect clusters additional to the oxygen precipitates. It is observed that the increase in the temperature of the HTHP treatment on samples  $S_5$ ,  $S_6$ , and  $S_4$  leads correspondingly to the increase in the size of these defect clusters (Fig. 5). It is important to note that these small defect clusters detected by selective etching, when of high concentration, mask the observation of the oxygen precipitates.

As one can see, the HTHP treatments of silicon samples lead to very complicated changes in the defect structure of the samples. The decrease in the oxygen concentration of samples  $S_2$ – $S_6$  in comparison with that of the untreated sample  $S_1$  is caused by the formation of oxygen precipitates during the HTHP treatments. The utilization of high pressure stimulates the precipitation process resulting in a higher concentration of oxygen precipitates in the silicon samples.<sup>15</sup> In other words, the lower the  $O_i$  concentration existing in the

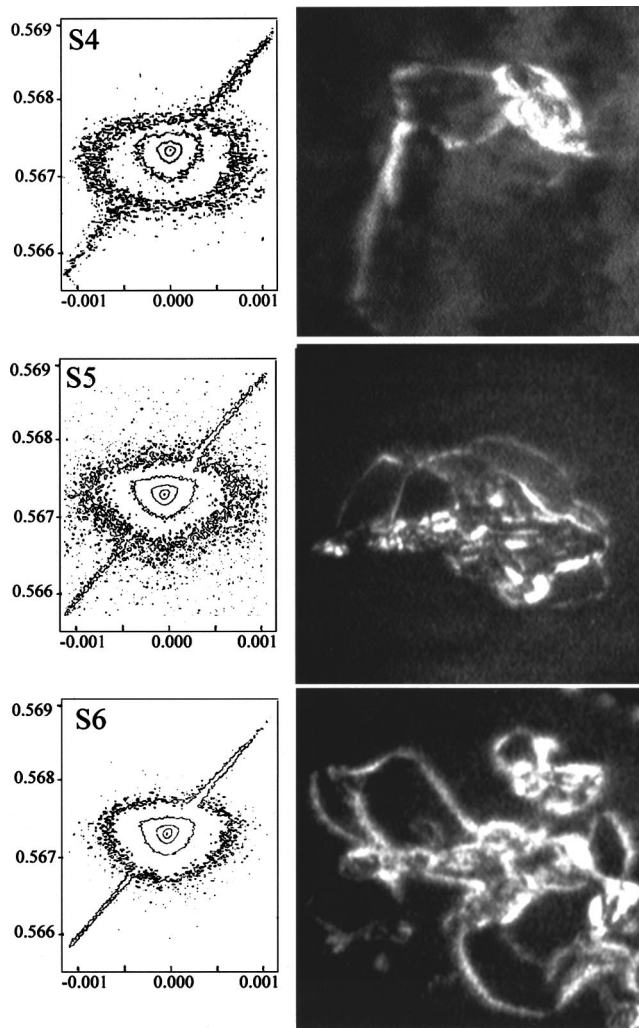


FIG. 4. Reciprocal space map around the 004 reciprocal space point (left) and plan-view TEM image (right) for samples  $S_4$ – $S_6$ . The axes are marked in  $\lambda/2d$  units,  $\lambda$  is wavelength and  $d$  is lattice interplanar distance. TEM image size is  $1 \times 0.75 \mu\text{m}$ .

samples after the HTHP treatments, the more oxygen precipitates are created. The self-interstitials liberated<sup>7</sup> during the formation of the oxygen precipitates are usually rejected<sup>16</sup> at the growing interface of the precipitate and the Si matrix. Along with this, other structural defects are formed<sup>17,18</sup> adjacent to the precipitates, like stacking faults and dislocation loops. These structural defects attract the self-interstitials. Thus, in our case, in the samples with more oxygen precipitates we shall have a higher number of self-interstitials produced, and therefore more self-interstitials could be rejected from the precipitates and collected in tangles of dislocation loops. These dislocation loops are formed adjacent to the precipitates if the temperature of the treatment is higher than  $850^\circ\text{C}$  for atmospheric pressure,<sup>19</sup> as well as for high pressure.<sup>13</sup> The self-interstitials collected at the dislocation loops most likely do not take part in the conversion process of the VO to the  $\text{VO}_2$  defect during the  $400^\circ\text{C}$  annealing stage, since the temperature that the self-interstitials are released from the dislocation loops cannot be lower than the temperature of the loop formation. But a part of the rejected self-interstitials can be present in the form of small clusters,

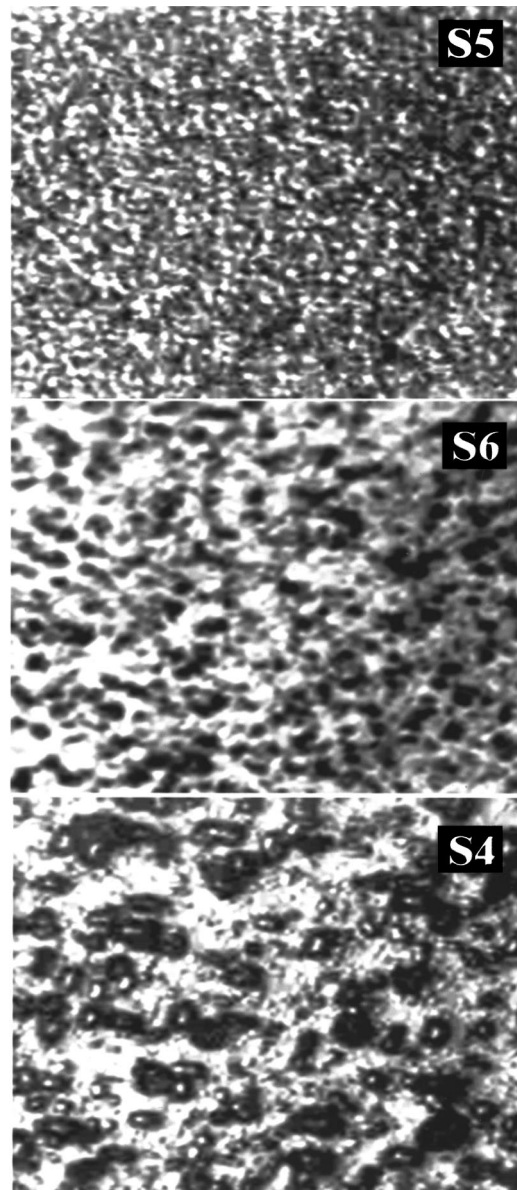


FIG. 5. Surface images after selective etching for samples  $S_5$ ,  $S_6$ , and  $S_4$  (from top to bottom).

which can have relatively low temperature stability. For example, di-interstitials are known to anneal<sup>20</sup> at  $400^\circ\text{C}$ . Notice that the neutron irradiation introduces high concentration of self-interstitials as well. They are expected to annihilate very effectively with vacancies at the first annealing stage (at  $220^\circ\text{C}$ ). Therefore the conversion of the VO defect to the  $\text{VO}_2$  defect will be determined by the remaining self-interstitials. Furthermore, as already mentioned, the selective etching studies show the additional formation of another kind of small defect cluster in the HTHP treated crystals (samples  $S_4$ – $S_6$ ). It is concluded that the concentration of the available self-interstitials in samples  $S_4$ – $S_6$  is decreased due to the treatments and therefore the contribution of the reactions (1) and (5) in the conversion process of the VO defect to the  $\text{VO}_2$  defect is reduced.

It is evident from the above discussion that due to the presence and the effect of the defects mentioned in the HTHP treated samples, a perfect fit of the experimental points and

the theoretical curves should not be expected. This is seen, for instance, in Fig. 1(a), which exhibits the variation of the  $N_{VO}$  versus the  $O_i$  concentration. In our analysis, the variations of the  $N_{VO}$  and the  $N_{VO_2}$  are described by a simple function of the  $O_i$  concentration [Eqs. (12) and (13), respectively]. In the fitting process we have chosen certain values for the parameters  $\alpha_1$ ,  $\alpha_2$ ,  $\alpha_3$ , and  $\alpha_4$ . This implies that  $N_{Si}$  and  $N_V$ , which are important for the fitting, also had constant values. This means that they were considered to be independent of the HTHP treatment. Generally, however,  $N_{Si}$  and  $N_V$  differ from one sample to another due to the different HTHP treatment they have been subjected to. These treatments in turn affect the  $O_i$  concentration. In other words, in handling the experimental data,  $N_{Si}$  and  $N_V$  ought to have been considered as functions of the  $O_i$  concentration. If that were taken into account, the conversion of the VO defect to the  $VO_2$  defect would most probably have led to a better fit of the experimental results than that described by Eqs. (12)–(14).

## CONCLUSIONS

It has been shown that HTHP treatments affect the annealing behavior of the VO defect. More specifically, HTHP treatments affect the concentration of the interstitial oxygen and the state of the self-interstitials adjacent to the precipitates, participating in the annealing of the VO defect. As a result, the particular contribution of the two main reactions  $VO + O_i \rightarrow VO_2$  and  $VO + Si_I \rightarrow O_i$  in the whole annealing process differs for each treatment, leading finally to different annealing behavior of the VO center in each sample. The formation of large dislocation loops adjacent to the oxygen precipitates in HTHP-treated samples means that only some of the rejected self-interstitials most likely take part in the

conversion of the VO to the  $VO_2$  defect. Thus this conversion is mainly affected by the decrease in the oxygen concentration due to the enhanced formation of the oxygen precipitates.

## ACKNOWLEDGMENTS

This work was supported in part by Polish Committee for Scientific Research (Grant No. 8T 11B 072 19). The help of M. Prujnszczyk from IET Warsaw with sample treatment is gratefully acknowledged.

- <sup>1</sup>J. W. Corbett, G. D. Watkins, and R. S. Mc Doland, *Phys. Rev.* **135**, A1381 (1964).
- <sup>2</sup>J. Lindstrom and B. Svenson, *Mater. Res. Soc. Symp. Proc.* **59**, 45 (1986).
- <sup>3</sup>C. A. Londos, N. V. Sarlis, and L. G. Fytros, *J. Appl. Phys.* **84**, 3569 (1998).
- <sup>4</sup>B. Pajiot, *Semicond. Semimetals* **42**, 191 (1994).
- <sup>5</sup>H. J. Stein, *Appl. Phys. Lett.* **48**, 1540 (1986).
- <sup>6</sup>R. C. Newman, *J. Phys.: Condens. Matter* **12**, R335 (2000).
- <sup>7</sup>R. C. Newman, *Semicond. Semimetals* **42**, 289 (1994).
- <sup>8</sup>H. Bender and J. Vanhellemont, in *Handbook in Semiconductors*, edited by S. Mahayan (1994), Vol. 3b, p. 1637.
- <sup>9</sup>A. Borghesi, B. Pivac, A. Sassella, and A. Stella, *J. Appl. Phys.* **77**, 4169 (1995).
- <sup>10</sup>K. Schmalz, K. Tittelbach, V. V. Emtsev, and Yu. N. Duluda, *Phys. Status Solidi A* **116**, K37 (1989).
- <sup>11</sup>U. Gosele, *Mater. Res. Soc. Symp. Proc.* **59**, 419 (1986).
- <sup>12</sup>R. C. Newman, *Mater. Res. Soc. Symp. Proc.* **104**, 25 (1988).
- <sup>13</sup>J. Jung and M. Lefeld-Sosnowska, *Philos. Mag.* **50**, 233 (1984).
- <sup>14</sup>A. Misiuk, *Phys. Status Solidi A* **171**, 191 (1999).
- <sup>15</sup>I. V. Antonova, A. Misiuk, V. P. Popov, A. E. Plotnikov, and B. Surma, *Physica B* **253**, 131 (1998).
- <sup>16</sup>F. A. Pouce and S. Hahn, *Mater. Sci. Eng., B* **4**, 11 (1989).
- <sup>17</sup>A. Bourret, J. Thisbault-Desseaux, and D. N. Seidman, *J. Appl. Phys.* **55**, 825 (1984).
- <sup>18</sup>K. Sawada, T. Karaki, and J. Watanabe, *J. Appl. Phys.* **53**, 6983 (1982).
- <sup>19</sup>H. Bender, *Phys. Status Solidi A* **86**, 245 (1984).
- <sup>20</sup>J. W. Corbett, J. C. Bourgoin, L. J. Cheng, J. C. Corelli, Y. H. Moonney, and C. Weigel, *Rad. Eff. Semicond., Conf. Ser.* **N31**, 1 (1976).